A literature review of FASERν

-An emulsion detector for collider neutrinos

Author: Lisa Andersson Loman
Supervisor: Else Lytken

Thesis submitted for Bachelor degree
Project conducted at half-speed during 4 months
Examination date: January 2021

LUND UNIVERSITY

Department of Physics
Division of Particle Physics

Abstract

In 2021, the ForwArd Search ExpeRiment (*FASER*) will start searching for light and weakly coupled particles $480\,m$ from the proton-proton collision point of ATLAS at the Large Hadron Collider (*LHC*). The FASER main detector will have a sub-detector, FASERν, sensitive to high-energy collider neutrinos of all flavours. This literature review of FASERν focuses on the neutrino program of FASER and apart from presenting the physics reach for FASERν it will also give an overview of the main experiment and the main detector. The flux of high-energy collider neutrinos and the number of neutrinos expected to interact in the detector is presented. The physics possibilities for FASER and FASERν are then discussed and an outlook for similar experiments is given.

Contents

Abbreviations

FASER ForwArd Search Experiment
ATLAS A Toroidal LHC ApparatuS
CERN Conseil Européen pour la Recherche Nucléaire
LHC Large Hadron Collider
pp proton-proton
IP interaction point
BSM Beyond the Standard Model
SM the Standard Model
CKM matrix Cabbibo-Kobayashi-Maskawa matrix
PMNS matrix Pontecorvo–Maki–Nakagawa–Sakata matrix
CC charged current
NC neutral current
$\boldsymbol{p_T}$ transverse momentum
LLP long-lived particle
HNL heavy neutral lepton
ALP axion-like particle
PMT photomultiplier tube
SCT semiconductor tracker
TPG thermal pyrolytic graphite
LHCb Large Hadron Collider beauty experiment
ECAL electromagnetic calorimeter
MIP minimum ionizing particle
LOS line-of-sight
HTS Hyper Track Selector
DIS deep inelastic scattering
DONuT Direct Observation of the Nu Tau
OPERA Oscillation Project with Emulsion-tRacking Apparatus
TAS Target Absorber Secondaries
TAN Target Absorber Neutral
FCC Future Circular Collider
HL LHC High Luminosity Large Hadron Collider

Chapter 1

Introduction

At the largest particle physics laboratory in the world, CERN, there is, in 2020, a new experiment under construction at the Large Hadron Collider (LHC). The ForwArd Search ExpeRiment ($FASER$) will be located 480 m from the ATLAS experiment proton-proton (pp) interaction point (IP) in the far forward direction and it will collect data during Run 3 of LHC in 2021-2023. As the FASER detector is currently being installed, this upcoming review thesis will only cover the preparatory part of the experiment.

FASER is dedicated to look for new, weakly coupled particles as well as neutrinos of all flavours, created at or near the ATLAS IP, at low transverse momenta (p_T). This thesis is a review project dedicated to briefly present FASER's search for new weakly coupled particles. Main focus of the text is on the project's neutrino program, FASERν. Following this introduction, chapter two presents the theoretical background to the physics supporting the FASER-project. Chapter three introduces the main experiment of FASER, which focuses on searching for light and very weak interacting particles that might produce dark matter with the correct relic density [1]. These particles are produced in the pp collision and travel in the forward direction (along the beam axis). Serendipitously, the chosen location for the FASER detector is also a possible location for detection of high-energy collider neutrinos. In a pp collision, neutrinos of all flavours are produced, but no neutrinos with high energy directly originating from a collision point have been detected — so far. With the addition of an emulsion detector, FASERν, the experiment aims to change this, something this thesis delves deeper into in chapter four. A discussion of all parts of the FASER project, including its neutrino experiment, is presented in chapter five. Chapter six covers the outlook and the thesis is concluded and summarized in chapter seven.

Chapter 2

Theoretical background

2.1 The Standard Model

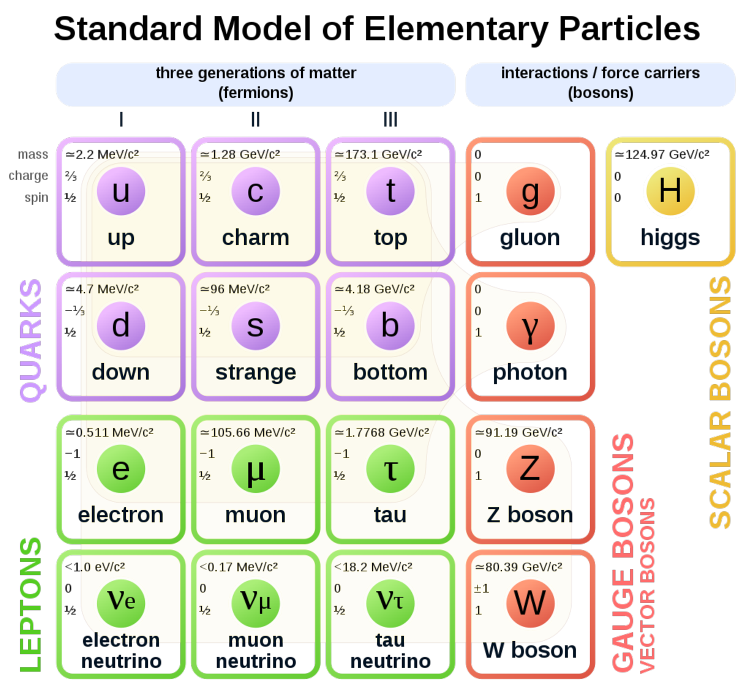

Figure 2.1: Schematic image of The Standard model of Elementary Particles [2].

The Standard Model (*SM*), which can be seen in figure 2.1, is a model containing the constituents of matter and force mediators between them. It is made up of two families called fermions with spin-1/2, namely the quarks and the leptons. The fermions follow Fermi-Dirac statistics and obey the Pauli exclusion principle.
There is also a family of bosons with spin-1 which obey Bose-Einstein statistics. These are the force mediators of the strong-, electromagnetic- and weak force and are called gluons, photons and W/Z-bosons respectively. Apart from these there is also the Higgs boson, which has spin-0 and is the boson giving mass to the elementary particles in the SM [3].

Leptons are spin-1/2 fermions without strong interactions. So far there are 6 known leptons divided into three generations with a doublet of leptons in each generation. Every generation contains a charged lepton and a neutrino of corresponding flavour as can be seen in figure 2.1. All leptons have anti-particles divided in the same manner. Neutrinos are leptons without charge and they have only been observed to interact via the weak force [3].

Neutrinos oscillate, meaning that neutrinos produced as one flavour state do not have to stay in that state but can change to a neutrino of a different flavour [4]. As it turns out, neutrinos interact as flavour eigenstates, but they propagate as the mass eigenstates ν_1, ν_2 and ν_3. In the book 'Introduction to Elementary Particles' [4], it is explained as the flavour eigenstates "are playing off each other, like the beats of a coupled oscillator". This behaviour is the same as can be seen for the quarks and the equivalent to the Cabbibo-Kobayashi-Maskawa matrix (*CKM* matrix) for quark mixing is the Pontecorvo–Maki–Nakagawa–Sakata matrix (*PMNS* matrix or *'MNS'* matrix as it is referred to in [4]) for neutrinos, where the weak eigenstates are used to define flavour:

$$\begin{pmatrix} \nu_e \\ \nu_\mu \\ \nu_\tau \end{pmatrix} = \begin{pmatrix} U_{e1} & U_{e2} & U_{e3} \\ U_{\mu1} & U_{\mu2} & U_{\mu3} \\ U_{\tau1} & U_{\tau2} & U_{\tau3} \end{pmatrix} \begin{pmatrix} \nu_1 \\ \nu_2 \\ \nu_3 \end{pmatrix} \tag{2.1}$$

Neutrino oscillations resolve the Solar Neutrino problem and this indicates that neutrinos have mass [4].

Apart from the fact that there are still sides of the neutrinos left to study, the SM does not give a solution to the dark matter problem and it does not explain the unbalance in the ratio between matter and anti-matter in the universe. Because of this, neutrino experiments and the search for new physics beyond the standard model (*BSM*) play a major role in the field of particle physics.

2.2 Weak interactions

In weak interactions the mediators are W^+, W^- and Z^0. These are all massive force mediators, consequently (by the Heisenberg uncertainty principle) the interaction has a very short range R. The mass of $W^\pm$ is $M_W = 80.4\, GeV/c^2$ and the Z^0 boson has mass $M_Z = 91.2\, GeV/c^2$ which for the W bosons leads to a range of;

$$R_W \equiv \frac{\hbar}{M_W c} \approx 2 \times 10^-3\, fm \tag{2.2}$$

The Z boson has a similar range since it has a similar mass. The derivation behind this can be seen for example in chapter 1.4 in [3].

The W and Z bosons couple to quarks and leptons. The strength of the weak coupling of $W^{\pm}$ is by convention set to $g_W/\sqrt{2}$ and gives the probability for a neutrino to emit a W^{+} boson and become an electron. g_W is the weak coupling constant with a value of $g_W = 1.166 \cdot 10^{-5}\, GeV^{-2}$ [5]. The strength of the coupling of $W^{\pm}$ is the same for all quarks and leptons.

Interactions where a $W^{\pm}$ is involved are called charged current (CC) reactions and for the Z^0 they are called neutral current reactions (NC). NC events are even more difficult to detect than CC events since the latter involves a transfer of electric charge as well as weak interaction charge while in a NC event a neutrino would remain a neutrino [5].

Chapter 3

ForwArd Search ExpeRiment

3.1 The experiment

So far the main focus on finding new physics at LHC has been on finding heavy particles (TeV masses) with $\mathcal{O}(1)$ couplings. FASER is, on the other hand, searching for light (MeV to GeV masses) and weakly coupled particles (new type of weak boson).

FASER is the result of the research conducted by a group dedicated to search for new physics that might be missed during current experiments at LHC. This refers to new particles that presumably are being produced during the collision but might not be noticed by the detectors close to the pp interaction points, where the detectors main target is set to find heavy particles with TeV-scale masses and large transverse momenta (p_T) [6][7].

However, there is a class of viable new particles that are light (MeV to GeV masses) and couple weakly to the SM [7]. Searching for these long-lived particles (LLP) at large p_T is not efficient since the SM cross sections are too small to produce enough particles in the direction with high transverse momentum. The scenario is different at low p_T, the cross section is much larger and therefore the number of particles produced in this direction is substantially higher. There is therefore a possibility to detect new, light and weak interacting particles with very low p_T in the forward direction.

The idea to look somewhere else than close to the IP for new particles is a resourceful way to use existing infrastructure to expand the physics possibilities while the search for heavy particles with high p_T continues. New theories that have emerged are explored to extend the reach of physics at LHC. If FASER is successful in finding new light and weakly-coupled particles, the energy range and size of the new detections could indicate dark matter with correct relic density and also explain the inconsistency between low-energy experiments and theoretical predictions [7].

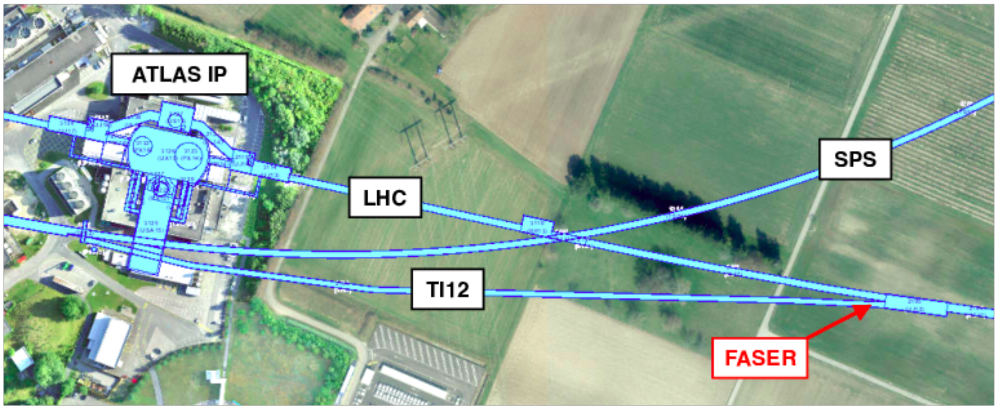

Figure 3.1: The location of FASER in relation to ATLAS IP and LHC [1].

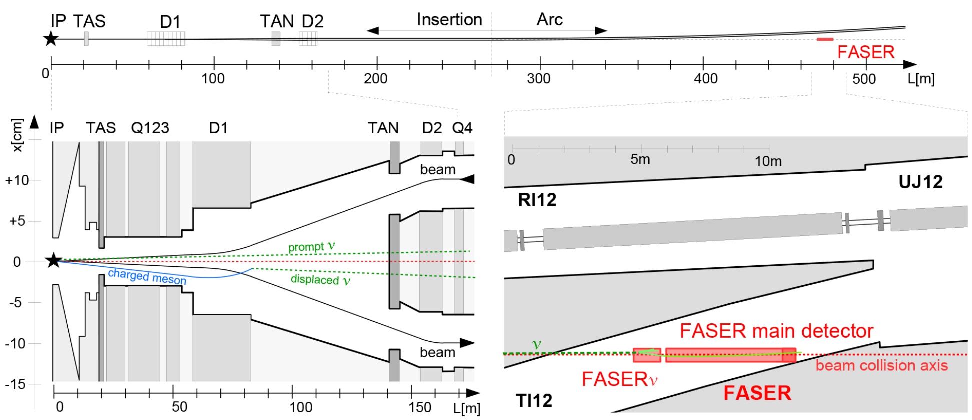

Figure 3.2: Schematic view of the FASER detector in tunnel TI12 [8].

In 2020, during LHC long shutdown 2, the FASER detector is being assembled in an unused service tunnel 480 m from the ATLAS IP, the location can be seen in figure 3.1. It is placed along the beam collision axis just after the beam optics have bent the charged particles [1]. There are multiple factors behind the decision for the location of the experiment, one of them being eliminating background data from SM events at the IP. If detectors were to be put in the forward direction immediately after the interaction, the background from SM events would be too high to be able to distinguish the result of the rare events involving the light and very weakly-coupled particles. However, since the particles of interest are light and weak interacting, they are long-lived and can therefore be detected several hundred meters away from the IP; and by making use of the existing shielding around ATLAS IP, most of the background has then been stopped by concrete and rock before reaching the intended location of the FASER detector. In this manner, the characteristics of the long-lived particle as well as the existing infrastructure, have been put into consideration when choosing the best possible location for the experiment. The remaining high-energy muons that are not filtered out on the path from the collision, will be vetoed by a double layer of scintillators in the detector [1].

Small emulsion detectors were placed in the tunnels TI12, the location chosen for the FASER detector, and TI18, an equidistant service tunnel on the other side of the ATLAS IP. Analysis of the results from these *in situ* measurements show that most of the background from the IP is filtered away [9].

One of the most interesting aspects of the detector is that FASER will use existing spare parts from other experiments at LHC [1]. By doing this the detector will be relatively inexpensive and therefore the financial risk of this experiment is low. The trackers which are used to separate and detect two high-energy, oppositely charged tracks (that can be traced back to the same location in the decay volume) are on indefinite loan from the ATLAS experiment. The calorimeter used to stop, identify and measure energies of high-energy electrons and photons comes from LHCb, is also loaned on the same premises. Hence the major construction cost will be the magnets in the detector.

Alongside the beyond the Standard Model (*BSM*) program searching for long-lived particles, FASER will also run a neutrino program which will be dedicated to study high-energy neutrinos originating from the pp collisions. This part of the experiment will hopefully uncover some of the mysteries concerning neutrinos and aims to be the first experiment to detect high-energy collider neutrinos. To be able to achieve this a sub detector called FASERν will be added to the main FASER detector. The sub detector is explained in detail in section 3.4 and the experiment neutrino program will be covered in more detail in chapter 4.

FASERν will measure interaction cross sections for high-energy collider neutrinos. Interaction cross sections are a measurement of how probable it is for a certain interaction to take place. Such measurements are useful when designing an experiment concerning neutrinos and interpreting results from neutrino oscillation experiments. The cross section indicates the number of neutrinos of a certain flavour that is expected to interact in a detector. It is of interest to have experimental measurements of interaction cross sections at high energies since it is also known that nuclear effects play a role at high energies.

The interaction cross sections of neutrinos are very small so to have a high flux of neutrinos entering the detector is of importance for the probability of neutrino interactions to be detected.

The differential cross section is the number of scattered particles per unit time and solid angle divided by the number of incoming particles per unit time and area [5];

$$\frac{d\sigma}{d\theta} = \frac{1}{\Phi \times N} \frac{dn}{d\theta} \tag{3.1}$$

Φ is the flux of incident particles per unit time and unit area and N is the number of scatterers in the target.

3.2 FASER's physics goals

FASER is aiming to find light weak interacting particles. A consequence of the weak coupling is that these particles can travel long distances through matter without interacting on their way. Hence they are long-lived particles.

These particles are produced at or close to the ATLAS IP, (equation 3.2) and move along the beam collision axis for $480\,m$ to the detector where they are visible through decay (equation 3.3) [10].

$$pp \to LLP + X \tag{3.2}$$

$$LLP \to \text{charged tracks} + X \ \big(\text{or } \gamma\gamma + X\big) \tag{3.3}$$

Presented below is a table of FASER's discovery prospects, including the discovery potential for the planned upgrade for FASER, FASER 2. However, the details of FASERS's discovery potentials regarding new weakly coupled particles is beyond the scope of this paper and a more detailed description of the FASER main experiment can be found in 'FASER's physics reach for long-lived particles' [7]. Details about the particles to possibly be discovered can be found in the references listed in the table.

Particles possible to detect	FASER	FASER 2	References
Dark Photons	yes	yes	[11]
B - L Gauge Bosons	yes	yes	[12]
Dark Higgs Bosons	-	yes	[13][14]
Heavy Neutral Leptons (*HNLs*) with e	-	yes	[15][16]
HNLs with μ	-	yes	[15][16]
HNLs with τ	yes	yes	[15][16]
Axion-Like Particles (*ALPs*) with Photon	yes	yes	[17]
ALPs with Fermion	yes	yes	[7]
ALPs with Gluon	yes	yes	[7]

Table 3.1: Presentation of the physics goals for FASER and the planned upgrade, FASER 2.

A high number of hadrons are produced at a pp collision point along the beam collision axis. Hadrons decay and produce a large flux of high-energy neutrinos. With the add-on of FASERν emulsion detector the physics reach is extended with the physics goals presented in table 3.2.

Physics goals for neutrino program achievable with FASERν
First experiment at LHC with a sensitivity to neutrinos
First detection of collider neutrinos
Detection of tau neutrinos
CC measurements of neutrino cross sections
Bound models of forward particle production
Constrain charm content of nucleon
Probe non-standard neutrino interactions (BSM physics)

Table 3.2: Presentation of the physics goals for FASERν.

The CC measurements of neutrino cross sections include identification of neutrino events and estimation of corresponding neutrino energy. Also noticeable is that this will be done in energy ranges where, in 2020, there are no measurements for neutrinos of either flavour. The first four physics goals in table 3.2 are treated more in chapter 4 of this thesis.

3.3 The main detector

The light new particles FASER is searching for are highly collimated around the beam axis. Because of this, there is no need for the detector to cover a large area [7]. Therefore the limited space in an unused side tunnel is enough to hold the detector setup. The location of the detector can be seen in figure 3.1 and 3.2 and the layout of the detector can be seen in figure 3.3. The entire detector will be roughly 1 m wide and 5 m long. Because of the small size of the detector, and the location of the unused service tunnel, only minor changes need to be made for the detector to align with the beam collision axis. One of these adjustments will be lowering the floor by 45 cm [7].

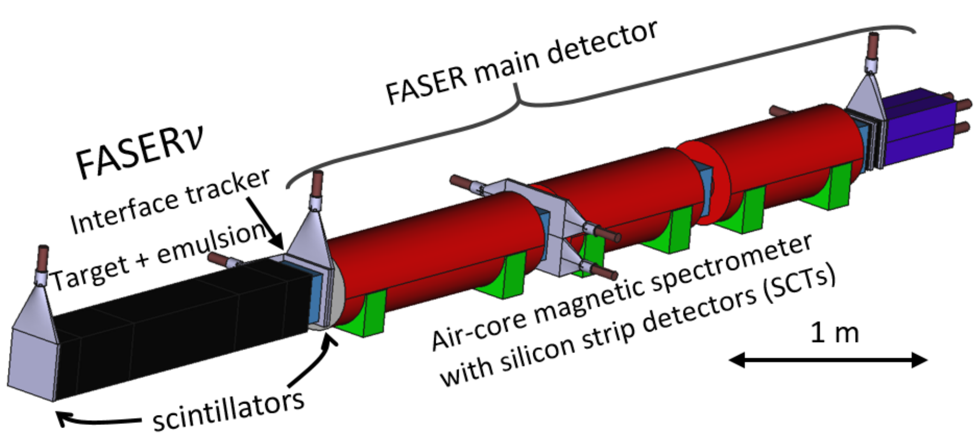

Figure 3.3: FASER main detector with the FASERν sub detector added to the front [8]. The particles will enter the detector from the left in the figure.

Scintillators

There are four scintillator stations in the main FASER detector which can be seen in grey in fig 3.3. They differ in design since they have different purposes in the detector.

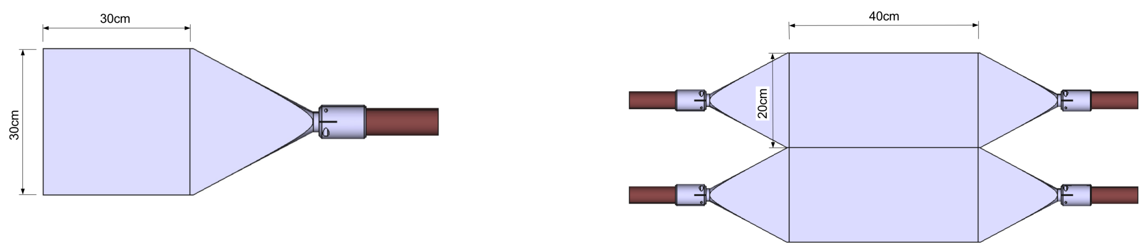

(a) Veto scintillator.

(b) Trigger scintillator.

Figure 3.4: Schematic image of scintillators to be used to veto charged particles and for trigger/timing in the FASER main detector [10].

The scintillators used for FASER are plastic scintillators and they fall under the category of organic scintillators. When a charged particle enters the scintillator material the ionizing radiation is absorbed and creates luminescence. I.e. the scintillator converts ionizing radiation into light. The light then passes through the light guide to the photomultiplier tube (PMT) where the scintillation photons are converted into electrons in the photocathode and the signal is amplified via the dynode system [18].

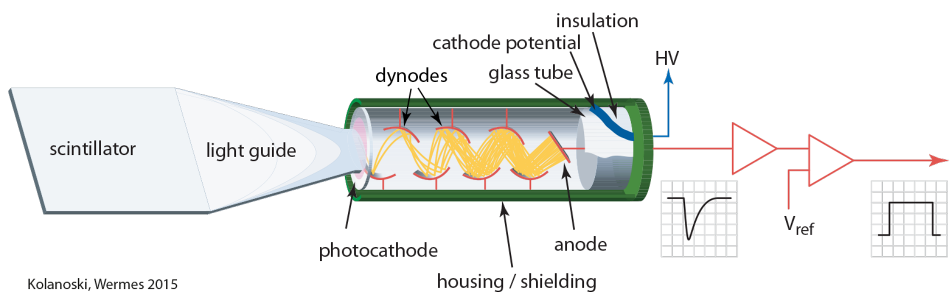

Figure 3.5: A plastic scintillator showing the scintillator, light guide and PMT [18].

The PMT will be enclosed in mu-metal to shield the sensitive process from magnetic fringe fields.

The veto scintillator's main purpose is to veto charged particles (background from high energy muons) from the IP when entering the detector. There are two identical scintillator stations for the veto purpose. In between these stations there is a block of concrete. The concrete is there to hinder energetic photons (that originates from muon bremsstrahlung before the detector) to enter undetected. The concrete will contain the photons or generate a shower that can be detected in the second veto station. The scintillator layers, which are $30\,cm \times 30\,cm \times 2\,cm$ can be seen in figure 3.4a. There are also scintillator layers used for trigger/timing in the detector. These are located after the first magnet and the calorimeter. The design of the scintillator stations for trigger/timing consists of a single scintillator layer made from two $20\,cm \times 40\,cm \times 1\,cm$ scintillator blocks which can be seen in figure 3.4b.

Magnets

As seen in red in figure 3.3 there are three magnets in the detector. The purpose and the location of FASER creates certain demands on the magnets. The dipole field needs to be large enough to separate pairs of oppositely charged particles originating from a common vertex in the decay volume. At the same time the magnet needs to be thin enough to fit the location in such a way that the line of sight is in the center of the detector. Another requirement is that power and cooling needs to be minimized, this is also due to space limitations and that the detector area is unavailable during the experiments. The same reasons apply for the weight and the size of the magnets when it comes to transporting parts through the tunnels to the detector area.

When it comes to the detector itself, the stray field of the magnets need to be small enough so that the PMTs used for the scintillator and calorimeter readout are not affected [10]. This is achieved by arranging permanent magnets in an Halbach array (see Fig. 3.6), which almost cancels the magnetic field outside the magnet.

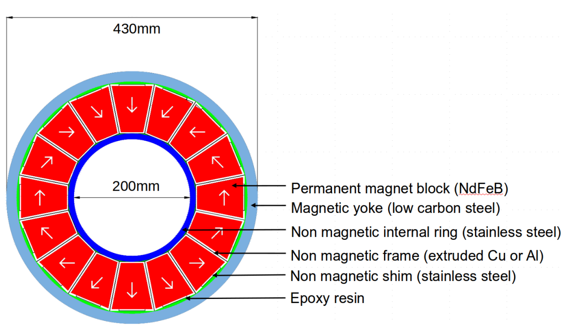

(a) Basic design of magnet to be used in FASER

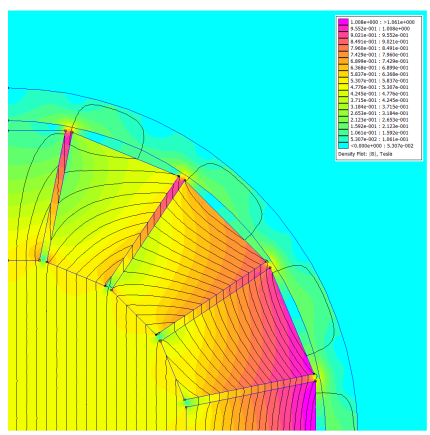

(b) Image of the field lines in the magnet

Figure 3.6: Schematic view of the $0.55\,T$ magnet for the FASER detector showing how the permanent magnets are arranged to create a dipole field [10].

Spectrometer/Tracker

A trackers role in a detector is to reconstruct the trajectories of the particles interacting in the detector. To be able to distinguish between two particles the separation needs to be $300\,\mu m$ [6], which is achieved by the magnetic field in the detector. FASER will be using an air-core magnetic spectrometer with three tracking stations using silicon strip modules

donated from the ATLAS experiment. The trackers consist of modules of semiconductor trackers (SCT) on indefinite loan from the ATLAS detector. They are located at the front, in the middle and at the end of the spectrometer. The three tracking stations are separated by two 1 m long, 0.55 T dipole magnets. At each tracking station there are three planes of SCT modules. The construction of each SCT module is two silicon strip detectors glued up back-to-back to a central thermal pyrolytic graphite (TPG) baseboard. The design is optimized to separate and detect two high-energy, oppositely charged tracks that share a common vertex in the decay volume. Another notable thing is that the interaction rate is much lower with respect to the ATLAS IP resulting in a trigger rate of $\sim 600\ Hz$. The low frequency of hits on the tracker leads to a simpler readout signal in this experiment in comparison to ATLAS. This leads to a different design of the readout system [10].
The cooling system is also different and in this case a water cooling system is used, which is enclosed in dry air to prevent condensation.

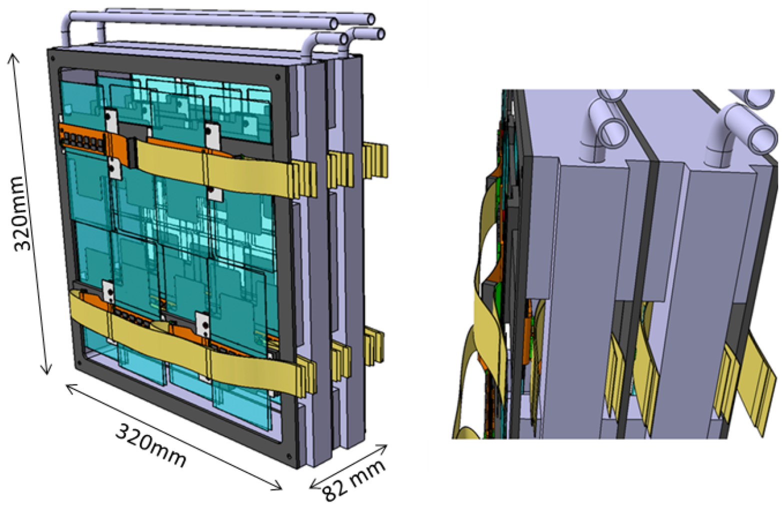

Figure 3.7: Schematic view of a tracking station. 8 SCT modules mounted in each plane and three planes mounted in a frame make up a tracking station. Visible in the image is also the cooling system (the tubes) and electronic connectors (in yellow) [10].

Apart from the change in readout system and cooling system no other major modifications are made. This saves time in the construction phase of FASER since most of the parts then can be re-used for the tracker planes.

The frame, to which the 8 modules per plane are attached, should be stable and have a minimum of 5 silicon strips overlap to ensure full geometrical coverage. It should also allow for water cooling system of the modules. ATLAS have agreed to allow FASER to use 80 spare SCT modules and the design of the tracker is based on this number [10].

Calorimeter

The electromagnetic calorimeter used in the FASER detector will stop high-energy electrons and photons as well as measure their energy. However, most events are pairs of high-energy photons or electron-positron pairs with such a small separation between the pairs that individual energy measurements will not be possible. Therefore the total energy of such pairs of particles will be measured.

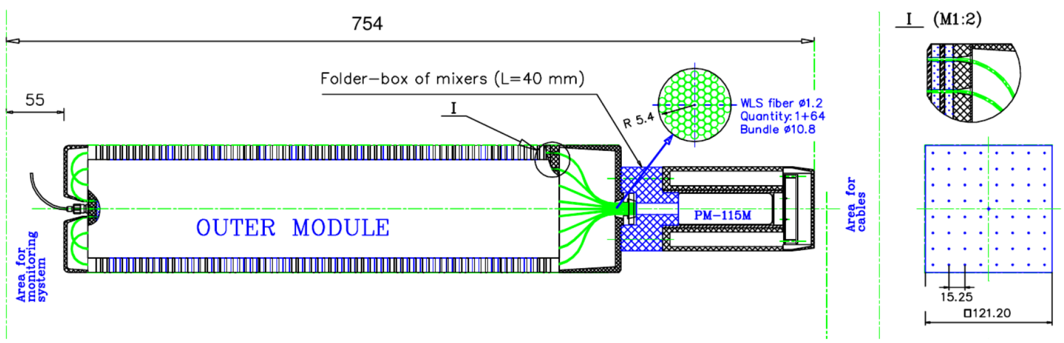

Figure 3.8: An LHCb outer ECAL module that will be used in FASER [10].

For the calorimeter, FASER will use four spare LHCb outer ECAL modules, shown in figure 3.8. The calorimeter has alternating layers of scintillators and lead plates. The size of the calorimeter (including the PMT) is 754 mm in length and has transverse dimensions of 121.2 mm by 121.2 mm, which covers the acceptance for FASER. All in all the calorimeter contains 66 layers of 2 mm lead and 4 mm plastic scintillator, resulting in a total depth of 25 radiation lengths. Radiation length is defined as the average thickness (in cm) of a material that reduces the mean energy by a factor e [3].

Trigger and data acquisition

For this experiment trigger and data acquisition is very important since the focus is to find evidence of very rare events. The trigger and data acquisition system has been designed to minimize the amount of equipment needed to be placed near the detector, since access is limited while the experiment is running and physical space is limited. The cables used will also be kept to a minimum since they need to be more than 500 m long, running between the IP and the detector [10].

3.4 Neutrino detector, FASERν

The detector will have an integrated luminosity of $150 fb^{-1}$, indicating that there is an expectation to find 150 events per femtobarn of cross section within the data from the 14 TeV LHC Run 3. This means that $2 \times 10^{11}\,\nu_e$, $6 \times 10^{12}\,\nu_\mu$ and $4 \times 10^{9}\,\nu_\tau$ as well as their respective anti-neutrinos will flow through FASERν. Assuming SM cross sections, the number of neutrinos interacting within the detector are expected to be $14000\,\nu_\mu$, $6000\,\overline{\nu}_\mu$, $14\,\nu_\tau$, $7\,\overline{\nu}_\tau$, $850\,\nu_e$ and $450\,\overline{\nu}_e$.

One requirement is that the detector should be sensitive to all three families of leptons produced by CC neutrino interactions. Another is that it needs a high spatial resolution to be able to distinguish between events. These requirements are both met by using an emulsion detector with a spatial resolution down to 50 nm.

The FASERν detector is an emulsion detector with a total of 1000 emulsion films interleaved with tungsten (target). The emulsion film is 70 μm thick on each side of a plastic base. The emulsion film consists of a gelatin media with silver bromide (AgBr) crystals with a size of 200 nm and each crystal works as an independent detection channel [8]. The density of the detection channels is therefore in the order of $10^{14}/cm^3$. This makes it possible to detect short-lived particles like tau leptons, which are needed to identify tau neutrino events.

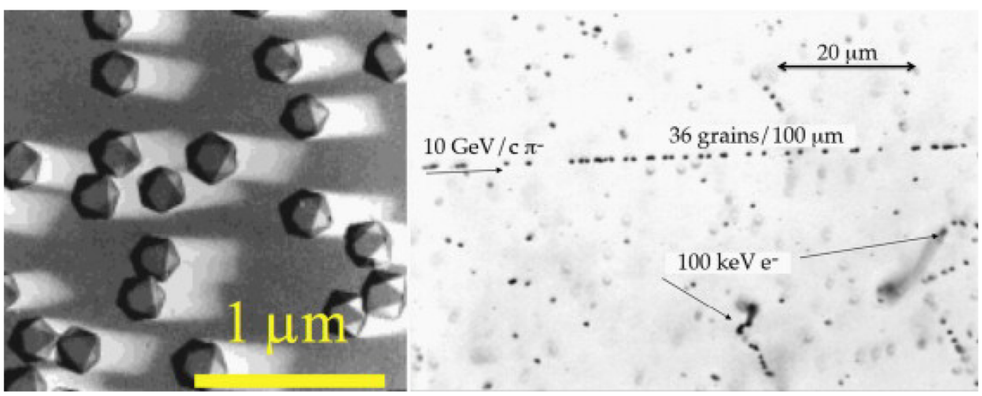

Figure 3.9: Image from 'Particle Detectors: Fundamentals and Applications' with a picture of AgBr crystals in an emulsion layer to the **left** and a track made by a minimum ionizing particle (MIP) to the **right** [18].

This emulsion detector is made up of 1000 layers of emulsion film with 1 mm tungsten in between each layer. Hence this $25\,cm \times 25\,cm \times 1.35\,m$ detector weighs 1.2 tons [8]. The FASERν neutrino detector will be placed in front of the FASER main detector, as shown in figure 3.3. It will be placed in the line-of-sight (LOS) of the IP to maximize the number of neutrino interactions.

An emulsion detector works in the same way as a photographic film. When the photosensitive emulsion layer is passed by an ionizing particle it leaves a track in the film, as can be seen to the right in fig 3.9. After development the track can be measured with very high resolution. This type of detector gives the highest spatial resolution compared to all other particle detectors available today [18].

In figure 3.10 the topology of the neutrino signals can be seen. Studying the topology of the neutrino signals will identify neutrino events in the emulsion detector. The classification of the different flavoured neutrino interactions is based on identifying the charged leptons e, μ and τ produced in the interactions and recorded in the emulsion film.

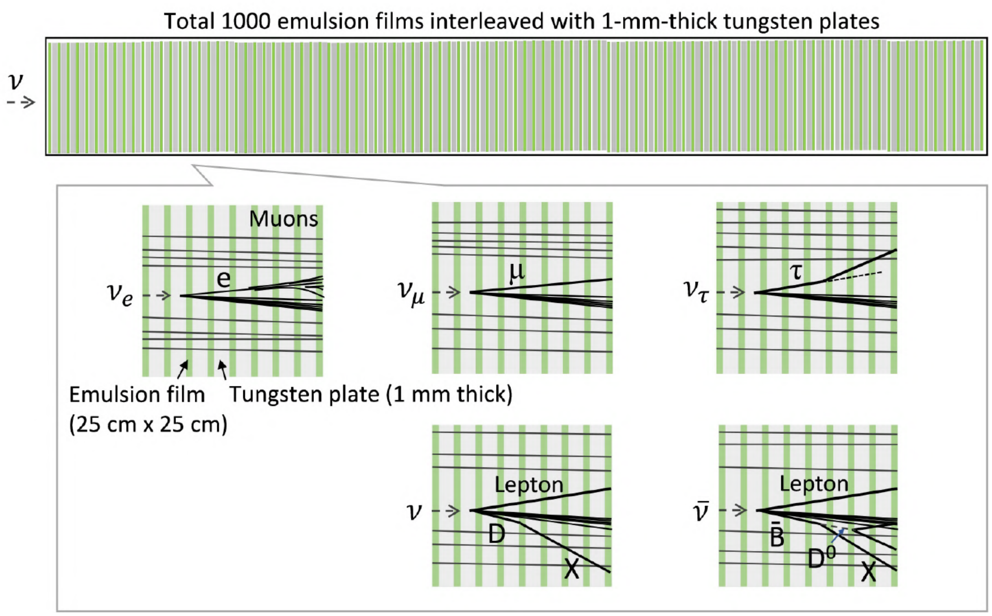

Figure 3.10: Side view of the layers in the emulsion detector and topology of the neutrino signals that is expected to be seen in the detector [8].

The thickness of the emulsion layers is a compromise between wanting the emulsion layer to be thick enough to provide useful information in one layer and to be thin enough to not be deformed during handling. The film is especially sensitive during the drying, after developing.

The materials for the layers in between the emulsion film modules have been chosen to keep the detector small and to localize electromagnetic showers in a small volume. With tungsten one can achieve this since the material has a high density and a short radiation length. In fact the length of the emulsion detector corresponds to 285 radiation lengths X_0 ($X_0 = 3.5\,mm$) and 10.1 hadronic interaction lengths λ_{int}. The radiation length refers to the energy lost in the material by electromagnetic interactions and the hadronic interaction length is how far a hadron can travel in a material before nuclear interaction occurs [19].

Since the emulsion detector lacks time resolution and records all charged particle trajectories, there will be a problem with pile-up. The crystals of silver bromide in the emulsion film are activated by particles travelling through. This process is what causes the tracks in the emulsion films which then can be analysed and identified. The emulsion film will be removed, analysed and replaced during technical stops every 3 months to keep the occupancy of the emulsion film low so that the events recorded in the emulsion film are distinguishable and is not too dense with muon tracks. The data recorded for each data-taking period is then corresponding to $10 - 50fb^{-1}$. Seven technical stops have been planned for run 3 of LHC which makes the total area of emulsion films add up to $440\,m^2$.

During these technical stops the emulsion detector needs to be replaced in four days or less. This has been taken into consideration when designing the detector since it needs to be replaced and transported easily to and from the detector location in a short amount of time.

Analysis and readout of the data

The first step of the analysis is then to readout the full area of the emulsion films, this will be done by using the Hyper Track Selector (HTS). The readout will then be carefully analysed to locate neutrino interactions. In figure 3.10 one can see a schematic image of the neutrino event tracks in the emulsion detector. Track position and direction is then measured.
The classification of the different flavoured neutrino's CC interactions are possible by identifying the products of that particular interaction. That is e, μ and τ leptons. The neutrino signals can be seen in figure 3.10.

The electron is identified by detecting electromagnetic showers along a track in the emulsion film, which can be seen in the image for ν_e in 3.10. If such a track is found, the film where the activity started is carefully examined. This is to see if only a single electron or an electron positron pair is causing the shower, since the latter would indicate π^0 decay with a γ conversion. By measuring their energy deposit (dE/dx) in the emulsion detector, particle pairs and single particles can be separated.

The muons are identified by the length of their tracks in the emulsion detector as shown in figure 3.10. All the hadrons from neutrino interaction will interact in the detector due to the nuclear interaction length ($10.1\,\lambda_{int}$), except for the ones created further downstream inside the detector. Also, the high density of muons crossing the neutrino detector will be used to align the detector with the line of sight of the beam collision axis.

The decay of the short lived tau lepton is used as an identifier for the tau neutrino and charm and beauty particles (with decay lengths of $c\tau \sim 100 - 500\,\mu m$). As can be seen in figure 3.10 there is a kink in the emulsion film that comes from the decay of tau lepton and the angle of this decay is used as a parameter for the identification of the tau neutrino.

There might also be a sign of some NC events but they are not considered in the analysis of the emulsion films.

Chapter 4

The neutrino program

This chapter will give a brief overview of the neutrino program of FASER, it is mostly based on the FASER Collaboration report 'Detecting and Studying High-Energy Collider Neutrinos with FASER at the LHC' [8] where more details can be found.

The neutrino was first discovered in a nuclear reactor in 1956 and since then neutrinos have been detected from numerous sources. Such as the Sun, cosmic ray interactions, beam dump experiments to mention a few. Neutrinos are also produced at particle colliders but so far they have not been detected. According to the FASER Collaboration's publication 'Detecting and studying High-Energy Collider Neutrinos with FASER at the LHC' [8] there are two main reasons for this. The first one being that neutrinos interact weakly, which makes neutrino interactions rare and difficult to detect above the background of other SM events. The second reason is that the neutrinos with the highest energy are produced along the beam line. As mentioned previously there are no detectors in that region since a detector here would hinder the beam of the collider.

Neutrino scattering in the deep inelastic scattering (DIS) regime, where energies are above $10\,GeV$, can provide access to lepton interactions with matter such as neutrino-parton interactions. There have been some high-energy neutrino measurements made, although none have been in the energy range considered for this experiment, that is in the range of $600\,GeV$ to $1\,TeV$.

The main production of neutrinos comes from hadron decays, which in turn are predominantly produced along the beam line. It is also known that the neutrinos behave similarly to the long-lived theoretical particles that FASER is aiming to detect. These two reasons together suggest that the location of the FASER detector is also ideal for a neutrino detector.

4.1 Physics goals

Neutrinos are produced with high numbers at colliders but none have been directly detected before. FASER has designed an experiment where this will be possible. The detector is placed on the beam collision axis - but far away enough for the background of SM events to be mostly filtered out. The detector will be sensitive to all three flavours of neutrinos and the individual flavours will be identified by analysing the lepton interaction tracks in the emulsion films of the detector. FASERν might also add significant data to what is known about ν_τ since only a handful of events with ν_τ have been detected in experiments so far.

The mean energies of the high-energy collider neutrinos are 600 GeV to 1 TeV depending on the flavour of neutrinos. The energies are above energies of previously detected man-made ν_τ and ν_e. For ν_μ there exist neutrino cross section measurements for lower energies from previous experiments (51. Neutrino Cross Section Measurements [20]) and for higher energies carried out by IceCube, which is a neutrino observatory in the South Pole where neutrinos from cosmic radiation are detected and studied. FASERν will therefore cover an energy range which for the time being has no measurements for neutrino cross sections.

Existing measurements for neutrino cross sections using neutrino-nucleon CC scattering can be seen in figure 4.1. Notice also that the energy spectras for FASERν all have peaks in a region where there are no measurements for cross sections.

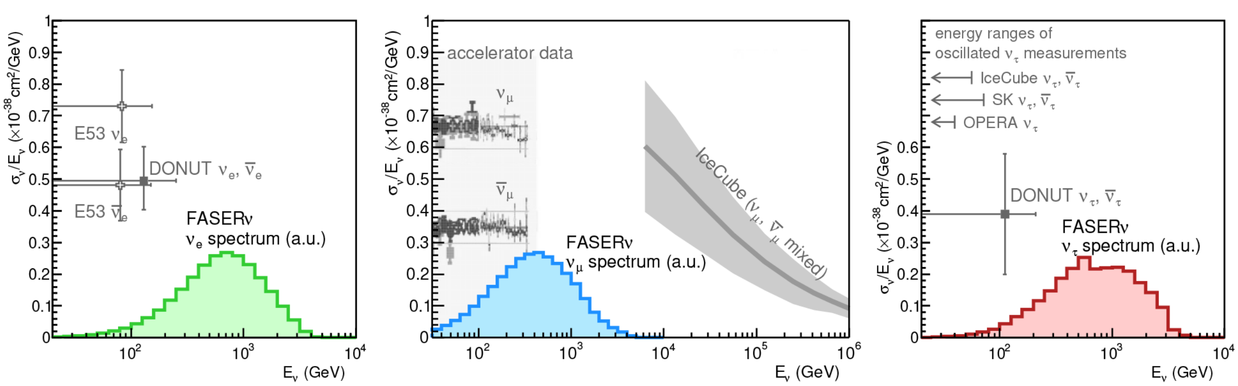

Figure 4.1: Existing measurements of νN CC scattering cross sections and expected energy spectra of neutrinos interacting with FASERν. N refers to an isoscalar nucleon in the target nucleus [8]. For ν_e (**left**) the existing measurements are from E53 [21] and DONuT [22]. For ν_μ (**middle**) there exists cross section measurements up to 360 GeV [20] and from 6.3 TeV and up [23]. For ν_τ(**right**) DONuT [22] is the only experiment who has reported a DIS cross section, measurements for oscillated ν_τ exists from IceCube [24], Super-Kamiokande [25] and OPERA [26] and the energy range of ν_τ cross sections are indicated in the plot.

One of the reasons for looking at cross sections at high energies is that experimental measurements of cross sections can help minimize systematic uncertainties in neutrino oscillation experiments, since nuclear effects play a major role at high energies. Also, if the measured cross sections for the three neutrino flavours where compared, this would provide a test of lepton universality in neutrino scattering. However, other experiments suggest violation of lepton universality in the decays $B \to D^*\ell\nu$ [27, 28, 29], $B \to K^*\ell\ell$ [30] and $B^+ \to K^+\ell\ell$ [31]. These results might originate from weak-scale physics and testing lepton universality in high energy neutrino scattering might help to exclude some theories regarding these flavour anomalies.

In this experiment it might also be possible to study the charm content of the nucleon and probe non-standard neutrino interactions. The latter might add a new entry to physics BSM [8].

4.2 Neutrino flux

One of the most important parts of the pre-work of FASERν is the estimation of neutrino flux. Since neutrinos are weak interacting a high flux of collider neutrinos are needed for the possibility of neutrinos interacting in the emulsion detector. This section gives an overview of what factors are taken into account when estimating the flux. More details and the exact models used can be found in 'Detecting and Studying High-Energy Collider Neutrinos with FASER at the LHC' [8] and FASERν Technical Proposal [9].

Neutrinos produced in the forward direction are mostly originating from hadron decays at the IP or further down the beam line. Where the neutrino production takes place is dependent on the lifetime of the hadron it originates from. When estimating the flux of neutrinos arriving at the FASERν detector it is therefore important to take SM hadron spectra as well as the infrastructure of LHC into consideration.

There are many hadronic interaction models developed to describe inelastic collisions in colliders and some of them were used here to simulate processes and obtain fluxes for a reliable estimation of the neutrino flux.

The need of different simulations are, among other things, a result from where the hadrons decay. For charm and beauty hadron decays, which occur close to the IP, a simulation using a Monte Carlo generator is sufficient. However, light and more long-lived hadrons decay further downstream from the IP. Hence a model of the propagation and absorption in the LHC beam pipe on their way towards FASER is needed.

Three major parts of infrastructure are to be treated with special consideration. The first part that the particle passes (as seen in figure 3.2) is the TAS front quadrupole absorber which essentially absorbs all hadrons with an angle of $\theta > 0.85\,mrad$. The hadrons from the IP also pass D1 which is a magnet with field strength of $3.5\,T$ which will deflect charged particles from their path on their way towards the FASER location. The third component is the TAN, a neutral particle absorber with a purpose to absorb photons and neutral hadrons.

In table 4.1 there is a list of the main decays considered in the estimations of neutrino production in the forward direction and more details on the simulations made for the neutrino flux can be found in 'Detecting and Studying High-Energy Collider Neutrinos with FASER at the LHC' [8].

Type of particle	Particles	Main decays
Pions	π^+	$\pi^+ \to \mu\nu$
Kaons	$K^+,\ K_S,\ K_L$	$K^+ \to \mu\nu,\ K \to \pi\ell\nu$
Hyperons	$\Lambda,\ \Sigma^+,\ \Sigma^-,\ \Xi^0,\ \Xi^-,\ \Omega^-$	$\Lambda \to p\ell\nu$
Charm	$D^+,\ D^0,\ D_s,\ \Lambda_c,\ \Xi_c^0,\ \Xi_c^+$	$D \to K\ell\nu,\ D_s \to \tau\nu,\ \Lambda_c \to \lambda\ell\nu$
Bottom	$B^+,\ B^0,\ B_s,\ \Lambda_b, ...$	$B \to D\ell\nu,\ \Lambda_b \to \Lambda_c\ell\nu$

Table 4.1: The table contains decays considered for the forward production of neutrinos at or close to the pp interaction point. Different simulation generators were used for the decays to get an estimation as accurate as possible.

The simulations are used to obtain neutrino flux as a function of energy with respect to the beam collision axis for all flavours. This statement implies that the neutrino flux is treated as being symmetric around the beam collision axis. In reality this symmetry might be broken by dipole magnets along the beam pipe though this effect is expected to be small and will therefore be disregarded.

For an integrated luminosity of $150\,fb^{-1}$ expected for Run 3 of $14\,TeV$ LHC from 2021-2023, the number of neutrinos streaming through FASERν is expected to be $2 \times 10^{11}\,\nu_e$, $6 \times 10^{12}\,\nu_\mu$ and $4 \times 10^{9}\,\nu_\tau$ as well as a comparing number of anti-neutrinos of respective flavours.

4.3 Neutrino interactions in FASERν

The interactions in this experiment can be described by deep inelastic scattering (DIS) since the energies of the neutrinos are $> 100\,GeV$. The differential cross section for neutrino scattering on protons therefore has the form;

$$\frac{d\sigma_{\nu p}}{dx\,dy} = \frac{G_F^2 m_p E_\nu}{\pi} \frac{m_{W,Z}^4}{(Q^2 + m_{W,Z}^2)^2} \times [x f_q(x, Q^2) + x f_{\bar{q}}(x, Q^2)(1-y)^2] \tag{4.1}$$

x is the fraction of the proton's momentum carried by the quark in the initial state and y is the fraction of the neutrino's momentum transferred to the hadronic system. $Q^2 = 2E_\nu m_p x y$ is the transferred four-momentum and $f_q(x, Q^2)$ is the proton parton distribution function. (this is further explained in [32] and [4]). For neutrino energies that are in the TeV range, the cross section peaks at $x \sim 0.1$, $y \sim 0.5$ and $Q^2 \sim (10\,GeV)^2$. So, in this energy range $Q^2 << m_{W,Z}^2$ and the corresponding neutrino interaction cross section is proportional to the neutrino energy $\sigma_{\nu N} \sim E_\nu$ which gives an energy spectrum of interacting neutrinos that peaks at higher energies.

FASERν will measure the interaction cross section of a neutrino hitting a tungsten nucleus and even though nuclear effects in heavy nuclei are important, they are not included in the analysis of the number of neutrino interactions in the detector. This is explained by having taken this into account by using nuclear parton distribution functions and noting that this only leads to very small changes in the calculations of the cross section. Therefore the cross section is given to be $\sigma_{\nu_N} = n_p\sigma_{\nu p} + n_n\sigma_{\nu n}$ where n_p and n_n are the number of protons and neutrons in the tungsten nucleus.

When calculating the probability of a neutrino to interact with the detector, a detector of pure tungsten is considered, that is without all the layers of emulsion film the actual detector will contain, since these are not expected to affect the calculations. Therefore only a pure tungsten block needs to be taken into account, so with a block of the size $25cm \times 25cm \times 1m$ and a density of $\rho = 19.3\, g/cm^3$ the total detector mass will be 1.2 tons, which is the same mass as the actual detector. This makes the probability to be:

$$P = \frac{\sigma_{\nu N} \times \text{Number of Nuclei}}{\text{detector area}} = \frac{\sigma_{\nu N}}{A}\frac{m_{det}}{m_N} = \sigma_{\nu N}\frac{\rho L}{m_N} \tag{4.2}$$

L is the length of the detector, m_{det} is the mass of the detector and m_N is the mass of the target nucleus N.

This is then used to calculate the number of neutrinos interacting with FASERν which is given by the product of the number of neutrinos passing the detector and the interaction probability. In table 4.2 the estimated number of neutrino interactions are presented.

	Number of CC interactions	Number of Reconstructed Vertices	Mean Energy
$\nu_e + \overline{\nu}_e$	1296^{+77}_{-58}	1037^{+52}_{-36}	$827\, GeV$
$\nu_\mu + \overline{\nu}_\mu$	20439^{+1545}_{-2314}	15561^{+1103}_{-1514}	$631\, GeV$
$\nu_\tau + \overline{\nu}_\tau$	$21^{+3.3}_{-2.9}$	$17^{+2.6}_{-2.6}$	$965\, GeV$

Table 4.2: Presented here is the number of estimated neutrino interactions in FASERν assuming pure tungsten detector, $14TeV$ run at LHC and an integrated luminosity of $150fb^{-1}$. Different simulation models have resulted in slightly different results which is reflected in the uncertainties. For the column 'Number of Reconstructed Vertices' a minimum of 5 charged tracks per vertex is required.

The number of neutrinos interacting are calculated as a function of neutrino angle and energy. It is given by the product of the number of neutrinos passing through FASERν and the probability for the neutrinos to interact in the detector.

4.4 Detection efficiency

By simulating neutrino energy using various models, topological and kinematic features of neutrino interactions as a function of the simulated energy enables identification of high-energy neutrino interactions. For example, high-energy neutrino interactions typically lead to a high number of charged tracks in the detector, originating from the interaction vertex. Taking this into account, a minimum of five charged tracks is required for a vertex when searching for high-energy neutrino interactions. This requirement is used for the number of reconstructed vertices in table 4.2 and results in a detection efficiency of above 80% for energies above $500\,GeV$.

As for the analysis of ν_τ, simulations show that one should require that τ crosses at least 1 emulsion film, the kink angle is bigger than 4 times the angular resolution and more than $0.5\,mrad$, and the flight length should be less than $6\,cm$, since the mean τ flight length is $3\,cm$. The last requirement is set to not confuse a ν_τ interaction with hadronic background. With these requirements detection efficiency is expected to be 75 %.

FASERν will not be able to distinguish between neutrinos and anti-neutrinos on its own. However, an additional interface detector, consisting of a silicon tracker layer (SCT modules from ATLAS), between FASERν and FASER main detector, as can be seen in figure 3.3, can solve this for the detection of muon neutrinos and anti-neutrinos. A combined analysis would be possible if an event from the emulsion detector is matched with an event in the interface detector. For electron neutrinos and tau neutrinos this would still be difficult since electrons make electromagnetic showers and taus decays mostly into hadrons, therefore their paths are not easy to follow. An interface detector would also improve the energy resolution and improve background rejection [9]. According to FASERν technical proposal [9], this interface detector is planned to be installed during the technical stop after the 2021 run, to have time to design the interface detector properly.

Chapter 5

Discussion

FASER is searching for light and extremely weak interacting particles that are very rare and difficult to detect. Since the experiment is still in the startup stage it is difficult to predict an outcome. There is no clear answer to where the solution to the dark matter issue will be found, but this small and relatively inexpensive experiment might give some hints about new physics and shed some light on where to look next.

The number of neutrinos expected to interact in FASERν is 20000 ν_μ, 1300 ν_e and 20 ν_τ, these numbers include both neutrinos and anti-neutrinos. The numbers are based on the integrated luminosity of 150 fb^{-1} for the 14 TeV LHC in 2021-2023, when FASER is expected to collect data. Since the estimations were made there has been some changes to the schedule due to the current corona virus pandemic [33][34]. The delays might be to the FASER project's advantage since they are on a tight schedule to get everything in order to start collecting data. However, the experiment itself might also be delayed for the same reasons, so only time can tell if the time plan for LHC Run 3 and FASER will coincide. One thing that might change is the installing of the interface detector between the main detector of FASER and the FASERν-addition since this was planned to be added after 2021 since more time is needed for the design process.

When FASERν is in place it can in theory start to collect data even before LHC is up and running. The emulsion detector can record neutrino interactions from cosmic radiation, therefore neutrino cross sections can be measured even without the presence of collider neutrinos.

When thinking about neutrino experiments it is easy to associate them with large-scale experiments, giant Cherenkov detectors like Super-Kamiokande (39.3 m in diameter and 41.4 m tall) or the IceCube detector which is 1 $(km)^3$ in size. FASERν is $25\,cm \times 25\,cm \times 1.35\,m$, that means that approxiamately 60000 FASERν detectors would fit in Super-Kamiokande and roughly 1.2×10^9 would cover the same volume as the IceCube detector. Though these experiments do not look for collider neutrinos or neutrinos in the same energy range, all three experiments are striving to unravel some of the mysteries concerning the weak interacting neutrinos.

If FASERν and FASER will be be able to reach the goals they have set up one could argue that it will lead the way for more small-scale experiments of this kind. Experiments where the existing environments are used to expand the physics reach to its full potential. Something that can be seen in many ways in these experiments, like when choosing the location, the size and the design of the detector etc.

Will the detection efficiency of the FASER's main detector be affected by the addition of FASERν? Since not much is known about the long-lived particles FASER is searching for this is a difficult question to answer. Of course it might be that some particles will decay in FASERν and therefore missed by the main detector, but it might also be so that they benefit from each other and data from matching events might help identify rare events. For example, concerning BSM searches, LLPs are both produced and decaying in the emulsion detector, which leads to a displaced vertex signal. The spatial resolution of FASERν can therefore probe decay lengths of $c\tau\gamma = 1\,mm$ to complement the searches for LLP in FASER with decay lenght $c\tau\gamma = 480\,m$. When an interface detector is added between FASER and FASERν, LLPs produced in the emulsion detector and decaying in the main detector decay volume might also be probed. If these originated from a neutral vertex in FASERν, it could indicate that the LLPs were in neutrino or dark matter interactions [8].

A point of critique towards FASER's BSM program might be that new physics can only be discovered if the collision energies of pp collisions are higher than the limitations of the LHC. In that case, there would be a need for a new and more powerful particle collider for new particles to be found, making experiments like FASER redundant since they would yield no useful results. Although CERN is planning to build a collider four times larger than LHC, the Future Circular Collider (FCC) will collect data in 2040 at the earliest [35], leaving decades to discover new physics with available means.

Chapter 6

Outlook

FASERν is the first experiment of its kind in many ways and the possibilities for opening new doors are many. For example, measuring the production of collider neutrinos in the forward direction. This is something that would be useful for any neutrino experiment at future colliders. FASERν is a small and relatively inexpensive neutrino experiment compared to giants like Super-Kamiokande and IceCube, this might show the physics community that large facilities are not required for doing neutrino physics. If successful in constraining neutrino cross sections it will reduce systematic uncertainties in neutrino oscillation experiments and other experiments with high-energy neutrinos. It might also open up to more collider neutrino experiments in the future.

An upgrade for FASER has been proposed. The upgrade, FASER 2, is aiming to search for LLPs at High Luminosity (*HL*) LHC - building on the experience of FASER. The new detector will also be located approximately 480 m from the ATLAS IP in the forward direction. It will have a decay volume of $\sim 10\,m^3$ hence extending the FASER project's sensitivity to detect particles by four orders of magnitude and the physics reach of HL LHC [36]. Some of the particles possible to detect with FASER 2 was also presented in table 3.1 of this thesis.

If the symbiosis of FASER's main detector and FASERν is considered beneficial, it might be that a similar addition will be a part of FASER 2 as well.

In addition to this, an upgrade for FASERν has recently been suggested, FASERν2 [37]. Proposed to be ten times the mass of FASERν, intended to be ready and start collecting data in 2026-27 at the HL LHC. Such a detector would be able to detect approximately $10^5\,\nu_e$, $10^6\,\nu_\mu$ and $10^3\,\nu_\tau$ originating from a pp collision point and having TeV energies. A location of the proposed detector has not been suggested.

Chapter 7

Conclusion

The ForwArd Search ExpeRiment will search for new, light and weakly coupled particles 480 m downstream from ATLAS proton-proton interaction point during Run 3 of LHC. This location is also ideal for detecting collider neutrinos for the first time with an added emulsion sub-detector, FASERν. The number of neutrinos streaming through FASERν is expected to be $2 \times 10^{11}\,\nu_e$, $6 \times 10^{12}\,\nu_\mu$ and $4 \times 10^{9}\,\nu_\tau$, as well as a comparing number of anti-neutrinos of respective flavours, for an integrated luminosity of 150 fb^{-1} expected for Run 3 of 14 TeV LHC from 2021-2023. This will result in a detection of approximately 1000 ν_e interactions, 15500 ν_μ interactions and 20 ν_τ. The different flavours of neutrino interactions will be classified by identifying the charged leptons in the interactions. Neutrino cross sections with a tungsten target will be measured by FASERν at previously unconstrained energies and FASERν will be the first experiment to detect high-energy collider neutrinos as well as detect tau neutrinos which is the least studied of the neutrinos.

In this thesis an overview of the FASER project has been presented with focus on the neutrino program of the experiment. This report is based on information and time plans available for Run 3 in the autumn of 2020. As 2020 has been a difficult year due to a corona virus pandemic some delays are to be expected that might be of advantage for the experiment.

Acknowledgement

I wish to acknowledge the invaluable support and guidance given by my supervisor Else Lytken throughout this project. Also, a special thanks to Josh Greaves and Jon Loman for giving great feedback in the process of writing.

Bibliography

[1] Ariga A, Ariga T, Boyd J, Cadoux F, Casper DW, Favre Y, et al. FASER: ForwArd Search ExpeRiment at the LHC. arXiv preprint arXiv:190104468. 2019.

[2] The Standard model of Elementary Particles; 2019. Last accessed 1 December 2020. Available from: https://commons.wikimedia.org/wiki/File:Standard$_{M}odel_{o}f_{E}lementary_{P}articles.svg$.

[3] Martin BR, Shaw G. Particle physics. John Wiley & Sons; 2017.

[4] Griffiths D. Introduction to elementary particles. John Wiley & Sons; 2008.

[5] Jönsson L. Lectures in Particle physics. Lunds universitet; 2010.

[6] Ariga A, Ariga T, Boyd J, Casper DW, Feng JL, Galon I, et al. Letter of Intent for FASER: ForwArd Search ExpeRiment at the LHC. arXiv preprint arXiv:181110243. 2018.

[7] Ariga A, Ariga T, Boyd J, Cadoux F, Casper DW, Favre Y, et al. FASER's physics reach for long-lived particles. Physical Review D. 2019;99(9):095011.

[8] Abreu H, Antel C, Ariga A, Ariga T, Boyd J, Cadoux F, et al. Detecting and studying high-energy collider neutrinos with FASER at the LHC. The European Physical Journal C. 2020;80(1).

[9] Abreu H, Andreini M, Antel C, Ariga A, Ariga T, Bertone C, et al. Technical Proposal: FASERnu. arXiv preprint arXiv:200103073. 2020.

[10] Ariga A, Ariga T, Boyd J, Cadoux F, Casper DW, Cerutti F, et al. Technical proposal for FASER: ForwArd Search ExpeRiment at the LHC. arXiv preprint arXiv:181209139. 2018.

[11] Feng JL, Galon I, Kling F, Trojanowski S. Forward search experiment at the LHC. Physical Review D. 2018;97(3):035001.

[12] Bauer M, Foldenauer P, Jaeckel J. Hunting all the hidden photons. Journal of High Energy Physics. 2018;2018(7):94.

[13] Feng JL, Galon I, Kling F, Trojanowski S. Dark Higgs bosons at FASER. arXiv preprint arXiv:171009387. 2017.

[14] Batell B, Freitas A, Ismail A, McKeen D. Flavor-specific scalar mediators. Physical Review D. 2018;98(5):055026.

[15] Kling F, Trojanowski S. Heavy neutral leptons at FASER. Physical Review D. 2018;97(9):095016.

[16] Helo JC, Hirsch M, Wang ZS. Heavy neutral fermions at the high-luminosity LHC. Journal of High Energy Physics. 2018;2018(7):56.

[17] Feng JL, Galon I, Kling F, Trojanowski S. ALPs at FASER: the LHC as a photon beam dump. arXiv preprint arXiv:180602348. 2018.

[18] Kolanoski H, Wermes N. Particle Detectors: Fundamentals and Applications. Oxford University Press, USA; 2020.

[19] Information on the absorption of hadrons; 2018. Last accessed 7 December 2020. Available from: https://twiki.cern.ch/twiki/bin/view/LHCb/TrackingEffAbsLength.

[20] Zyla PA, et al. Review of Particle Physics. PTEP. 2020;2020(8):083C01.

[21] Baker NJ, Kahn SA, Murtagh MJ, Samios NP, Tanaka M, Baltay C, et al. $\nu_\mu - \nu_e$ universality in charged-current neutrino interactions. Phys Rev D. 1990 May;41:2653–2666. Available from: https://link.aps.org/doi/10.1103/PhysRevD.41.2653.

[22] Kodama K, Ushida N, Andreopoulos C, Saoulidou N, Tzanakos G, Yager P, et al. Final tau-neutrino results from the DONuT experiment. Physical Review D. 2008;78(5):052002.

[23] Robertson S. Measurement of the multi-TeV neutrino cross section with IceCube using Earth absorption. arXiv preprint arXiv:190806123. 2019.

[24] Aartsen M, Ackermann M, Adams J, Aguilar J, Ahlers M, Ahrens M, et al. Measurement of atmospheric tau neutrino appearance with IceCube DeepCore. Physical Review D. 2019;99(3):032007.

[25] Li Z, Abe K, Bronner C, Hayato Y, Ikeda M, Iyogi K, et al. Measurement of the tau neutrino cross section in atmospheric neutrino oscillations with Super-Kamiokande. Physical Review D. 2018;98(5):052006.

[26] Agafonova N, Alexandrov A, Anokhina A, Aoki S, Ariga A, Ariga T, et al. Final Results of the OPERA Experiment on ν τ Appearance in the CNGS Neutrino Beam. Physical review letters. 2018;120(21):211801.

[27] Lees J, Poireau V, Tisserand V, Grauges E, Palano A, Eigen G, et al. Measurement of an Excess of B→ D (*) τ- ν τ Decays and Implications for Charged Higgs Bosons. Physical Review D. 2013;88(7):072012.

[28] Hirose S, Iijima T, Adachi I, Adamczyk K, Aihara H, Al Said S, et al. Measurement of the τ Lepton Polarization and R (D^*) in the Decay $\bar{B} \rightarrow$ D$^*\tau^-$ $\bar{\nu}_\tau$. Physical Review Letters. 2017 05;118.

[29] Aaij R, Adeva B, Adinolfi M, Ajaltouni Z, Akar S, Albrecht J, et al. Measurement of the ratio of the B 0→ D*- τ+ ν τ and B 0→ D*- μ+ ν μ branching fractions using three-prong τ-lepton decays. Physical review letters. 2018;120(17):171802.

[30] Aaij R, Adeva B, Adinolfi M, Ajaltouni Z, Akar S, Albrecht J, et al. Test of lepton universality with B 0→ K* 0 + - decays. Journal of High Energy Physics. 2017;2017(8):55.

[31] Aaij R, Beteta CA, Adeva B, Adinolfi M, Aidala CA, Ajaltouni Z, et al. Search for lepton-universality violation in B+→ K+ + - decays. Physical review letters. 2019;122(19):191801.

[32] Kane G. Modern elementary particle physics: explaining and extending the standard model. Cambridge University Press; 2017.

[33] Schaeffer A. New schedule for CERN's accelerators and experiments; 2020. The schedule for the current long shutdown (LS2) has had to be modified due to the COVID-19 pandemic. Available from: https://home.cern/news/news/accelerators/new-schedule-cerns-accelerators-and-experiments.

[34] Schaeffer A. A new schedule for the LHC and its successor; 2019. The LHC will restart in May 2021 and Run 3 will be extended by one year. Available from: https://home.cern/news/news/accelerators/new-schedule-lhc-and-its-successor.

[35] International collaboration publishes concept design for a post-LHC future circular collider at CERN; 2019. Last accessed 13 December 2020. Available from: https://home.cern/news/press-release/accelerators/international-collaboration-publishes-concept-design-post-lhc.

[36] Collaboration F. FASER 2: Forward Search Experiment at the HL LHC; 2020. Last accessed 9 December 2020. Available from: https://www.snowmass21.org/docs/files/summaries/EF/SNOWMASS21-EF9$_EF6 - NF3_NF6 - RF6_RF0 - CF7_CF0 - AF5_AF0_FASER2 - 038.pdf$.

[37] Collaboration F. FASERν 2: A Forward Neutrino Experiment at the HL LHC; 2020. Last accessed 9 December 2020. Available from: https://www.snowmass21.org/docs/files/summaries/NF/SNOWMASS21-NF10$_NF6 - EF6_EF9 - IF0_FASERnu2 - 006.pdf$.